Research Article | Vol. 8, No. 10 | 1 Oct 2018 | OPTICAL MATERIALS EXPRESS 3072
Optical Materials EXPRESS

Composite polymer membranes for laser-induced fluorescence thermometry

FRANCISCO GONZÁLEZ-MARTÍNEZ,[1] OSCAR GONZÁLEZ-CORTEZ,[1] REINHER PIMENTEL-DOMÍNGUEZ, [1] JUAN HERNÁNDEZ-CORDERO,[1,*] AND GUILLERMO AGUILAR[2]

[1]*Instituto de Investigaciones en Materiales, Universidad Nacional Autónoma de México, Ciudad Universitaria, Coyoacán, Ciudad de México 04510, México*
[2]*Department of Mechanical Engineering, University of California Riverside, Riverside, CA 92521, USA*
**jhcordero@iim.unam.mx*

Abstract: We demonstrate a modified version of laser-induced fluorescence thermometry (LIFT) for mapping temperature gradients in the vicinity of small photothermal devices. Our approach is based on temperature sensitive fluorescent membranes fabricated with rhodamine B and polydimethylsiloxane (PDMS). Relevant membrane features for LIFT, such as temperature sensitivity, thermal quenching and photobleaching are presented for a range of 25 °C to 90 °C, and their performance is evaluated upon obtaining the temperature gradients produced in the proximity of optical fiber micro-heaters. Our results show that temperature measurements in regions as small as 750 µm x 650 µm, with a temperature resolution of 1 °C, can be readily obtained.

OCIS codes: (160.4670) Optical materials; (160.5470) Polymers; (160.2540) Fluorescent and luminescent materials; (350.5340) Photothermal effects; (100.2960) Image analysis.

References and links

1. E. Samiei, M. Tabrizian, and M. Hoorfar, "A review of digital microfluidics as portable platforms for lab-on a-chip applications," Lab Chip **16**(13), 2376–2396 (2016).
2. M. M. Kim, A. Giry, M. Mastiani, G. O. Rodrigues, A. Reis, and P. Mandin, "Microscale thermometry: A review," Microelectron. Eng. **148**, 129–142 (2015).
3. V. K. Natrajan and K. T. Christensen, "Fluorescent Thermometry," in *Encyclopedia of Microfluidics and Nanofluidics*, D. Li, ed. (Springer, 2015).
4. P. Löw, B. Kim, N. Takama, and C. Bergaud, "High-spatial-resolution surface-temperature mapping using fluorescent thermometry," Small **4**(7), 908–914 (2008).
5. D. Ross, M. Gaitan, and L. E. Locascio, "Temperature measurement in microfluidic systems using a temperature-dependent fluorescent dye," Anal. Chem. **73**(17), 4117–4123 (2001).
6. R. Fu, B. Xu, and D. Li, "Study of the temperature field in microchannels of a PDMS chip with embedded local heater using temperature-dependent fluorescent dye," Int. J. Therm. Sci. **45**(9), 841–847 (2006).
7. V. K. Natrajan and K. T. Christensen, "Two-color laser-induced fluorescent thermometry for microfluidic systems," Meas. Sci. Technol. **20**(1), 015401 (2009).
8. P. Chamarthy, S. V. Garimella, and S. T. Wereley, "Measurement of the temperature non-uniformity in a microchannel heat sink using microscale laser-induced fluorescence," Int. J. Heat Mass Transfer **53**(15-16), 3275–3283 (2010).
9. J. Wu, T. Y. Kwok, X. Li, W. Cao, Y. Wang, J. Huang, Y. Hong, D. Zhang, and W. Wen, "Mapping three-dimensional temperature in microfluidic chip," Sci. Rep. **3**(1), 3321 (2013).
10. W. Jung, Y. W. Kim, D. Yim, and J. Y. Yoo, "Microscale surface thermometry using SU8/Rhodamine-B thin layer," Sensors Actuator A **171**(2), 228–232 (2011).
11. S. Ebert, K. Travis, B. Lincoln, and J. Guck, "Fluorescence ratio thermometry in a microfluidic dual-beam laser trap," Opt. Express **15**(23), 15493–15499 (2007).
12. D. Moreau, C. Lefort, R. Burke, P. Leveque, and R. P. O'Connor, "Rhodamine B as an optical thermometer in cells focally exposed to infrared laser light or nanosecond pulsed electric fields," Biomed. Opt. Express **6**(10), 4105–4117 (2015).
13. L. Gui and C. L. Ren, "Temperature measurement in microfluidic chips using photobleaching of a fluorescent thin film," Appl. Phys. Lett. **92**(2), 024102 (2008).
14. G. Y. Zhuo, H. C. Su, H. Y. Wang, and M. C. Chan, "In situ high-resolution thermal microscopy on integrated circuits," Opt. Express **25**(18), 21548–21558 (2017).

#335486 https://doi.org/10.1364/OME.8.003072
Journal © 2018 Received 20 Jun 2018; revised 17 Aug 2018; accepted 18 Aug 2018; published 11 Sep 2018

Optical Materials EXPRESS

15. L. V. J. Behm, I. Schlenther, M. Petrausch, F. Jorde, N. Godino, F. Pfisterer, C. Duschl, and M. Kirschbaum, "A simple approach for the precise measurement of surface temperature distributions on the microscale under dry and liquid condition based on thin Rhodamine B films," Sens. Actuators B Chem. **255**, 2023–2031 (2018).
16. M. P. Wolf, G. B. Salieb-Beugelaar, and P. Hunziker, "PDMS with designer functionalities-properties, modifications strategies, and applications," Prog. Polym. Sci. **83**, 97–134 (2018).
17. R. Pimentel-Domínguez, P. Moreno-Álvarez, M. Hautefeuille, A. Chavarría, and J. Hernández-Cordero, "Photothermal lesions in soft tissue induced by optical fiber microheaters," Biomed. Opt. Express **7**(4), 1138–1148 (2016).
18. R. Pimentel-Domínguez, A. M. Velázquez-Benítez, J. R. Vélez-Cordero, M. Hautefeuille, F. Sánchez-Arévalo, and J. Hernández-Cordero, "Photothermal effects and applications of polydimethylsiloxane membranes with carbon nanoparticles," Polymers (Basel) **8**(4), 84 (2016).
19. G. Liu, Q. Sheng, D. Dam, J. Hua, W. Hou, and M. Han, "Self-gauged fiber-optic micro-heater with an operation temperature above 1000°C," Opt. Lett. **42**(7), 1412–1415 (2017).

1. Introduction

The advent of new microanalysis platforms, such as lab on a chip and microfluidic systems, has triggered extensive research aimed at studying thermal phenomena at the micron scale [1]. Given the size of these systems, phenomena such as heat transfer and heat loss to the surrounding media become relevant for most practical applications (e.g., DNA replication, electronic cooling, thermal generation of pH gradients [2]) and are of paramount interest for characterization and optimization purposes. In addition to temperature measurements, it is often desirable to obtain a temperature map, which could provide useful information related to thermal phenomena occurring in the system and its vicinity [1,2]. In general, a 'micro-thermometer' should be able to provide high spatial resolution, high acquisition rate for real-time sampling, low thermal inertia for rapid response and adequate temperature resolution. Among these features, measurements with high spatial resolution are perhaps the most challenging to obtain.

Several methods have shown to provide high spatial resolution (<1 μm) temperature measurements achieving thermal resolutions of less than <0.1 °C [2]. Contact techniques, involving the use of devices such as scanning thermal probes or micro- and nano-thermocouples, provide an effective means to obtain local temperature measurements with spatial resolutions of up to 0.01 μm [2]. Non-contact techniques, albeit more elaborated and expensive, can yield a two-dimensional temperature map with high spatial resolution (e.g., 0.1 μm with infrared thermometry) and accuracy (e.g., 1 μK with laser interferometry) [2]. Among the different non-intrusive techniques available, fluorescent thermometry is one of the most widely used owing to its relative simplicity using commercially available cameras (CCD or CMOS); it can further be adapted to a microscope to obtain high spatial resolution measurements [3,4]. Temperature measurements rely on a fluorophore, typically a dye whose fluorescent intensity decreases with temperature, which can be either dissolved in a fluid or deposited on a surface of interest [4–6]. Excitation of the fluorophore is customarily done with laser light; hence, the technique is termed laser-induced fluorescence thermometry (LIFT). The spatial resolution depends on the imaging optics whereas the temporal resolution is defined by the framing rate of the camera. Successful applications of LIFT include temperature mapping of microfluidic channels [7–9], characterization of electrical microheaters [10] and thermal mapping of an optical trap [11], to name a few.

Rhodamine B (RhB) is the most widely used dye for LIFT, and its fluorescence intensity strongly depends on the solvent [3–10]. Water and ethanol based solutions are the most common choices for temperature measurements in liquid samples, although other solvents such as sodium carbonate buffer solutions have also shown to perform well [5,6,11,12]. For temperature mapping of dry surfaces, RhB can also be incorporated into polymer matrices to fabricate temperature sensitive films [9,10,13–15]. In particular, integration of RhB into polydimethylsiloxane (PDMS) is of interest because of its dominant role in microfluidic and lab-on a-chip platforms [16]. In this work, we show a simple method for fabricating temperature sensitive PDMS membranes with RhB for LIFT. The PDMS-RhB composite is obtained by simple mixing and is subsequently molded and cured to yield large membranes

Optical Materials EXPRESS

that can be cut down to a convenient size. The membranes can be easily placed in direct contact with the sample or device of interest and the temperature map can then be obtained through fluorescence image analysis. We analyze the performance of the membranes as temperature sensitive elements for LIFT, within a range from 25 °C to 90 °C, and demonstrate their application for characterization of photothermal devices fabricated with standard single-mode optical fibers [17].

2. Experiments

2.1 Fabrication of PDMS-RhB membranes

The PDMS-RhB membranes were fabricated with Rhodamine B (Sigma Aldrich, R6626) incorporated into PDMS (Dow Corning, Sylgard 184). We followed a procedure similar to that previously reported for fabricating PDMS membranes with embedded carbon nanoparticles [18]. Briefly, RhB was added in the base material of the PDMS with a concentration of 0.1% in weight; the solution was mixed with chloroform (0.75 ml of chloroform per gram of base material) using a magnetic stir bar for 120 minutes at room temperature. The mixture was subsequently heated at 70 °C to completely evaporate the chloroform and then further mixed by hand for 5 minutes to incorporate the PDMS curing agent in a 1:10 ratio. The resulting PDMS-RhB composite was then poured into custom made glass slide molds and cured at 60 °C for 24 hours. After cooling, the resulting PDMS-RhB membranes were removed from the mold yielding samples with smooth surfaces.

2.2 Temperature control

For temperature control and calibration, we used a setup comprising a thermoelectric cooler (Thorlabs, TEC3-6), a ceramic resistive heater (Thorlabs, HT24S) and a thermistor (Thorlabs, TH10K). These elements were mounted on a heat sink and enclosed in a thermally insulating material. A PID controller (Thorlabs, TED200C) was used in the setup allowing for controlling the temperature from 15 to 120 °C with 0.1 °C precision.

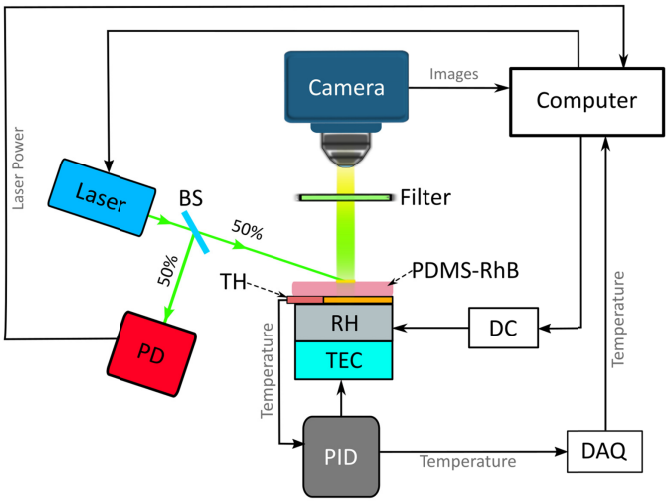

Fig. 1. Setup for laser-induced fluorescence imaging: a photodetector (PD) was used for monitoring the stability of the laser; synchronization, temperature control, image acquisition and processing were done via a personal computer. PID: proportional-integral-derivative controller; TEC: Thermoelectric cooler; RH: ceramic heater; TH: thermistor; BS: beam splitter. The laser beam is expanded by a lens (not shown) to increase the illumination area.

Optical Materials EXPRESS

2.3 Laser-induced fluorescence thermometry setup

The setup for LIFT measurements comprised a CW diode-pumped solid-state green laser (532 nm, BWTEK, model BWI532-50-E, beam diameter < 1 mm) with ± 3% power stability. The illumination area is increased by a lens (10x, NA 0.25) yielding a spot size of approximately 2 cm. Images are acquired using a CMOS camera (Thorlabs, DCC1645C) with a 10x microscope objective (see Fig. 1). A notch filter (533 nm, 17 nm FWHM, Thorlabs, NF533-17) was further used to eliminate the green radiation in the images recorded by the camera. As seen in Fig. 1, a 50% beam splitter was used to simultaneously excite with the laser the fluorescence of the PDMS-RhB membranes and for monitoring power fluctuations. The latter was done by means of an optical power meter and a thermal power sensor (Thorlabs, S302C). Data from the sensor allowed us to account for spurious effects of laser power fluctuations that typically require using two dyes (one of them temperature insensitive) or two cameras [7,8]. Our modified version for LIFT allowed for minimizing these effects simply by taking the intensity ratio of the images to that registered by the sensor. More details of this normalization process are provided below.

For temperature calibration, the membranes were placed on the ceramic heater and the temperature was set to a desired value. Fluorescence images were then acquired and post-processed to yield the calibration curves (i.e., normalized intensity vs. temperature) for the membranes. For all measurements, the camera gain was adjusted manually and kept constant. The resulting curves were then used to obtain the temperature maps across the membranes; with this setup, the spatial resolution of the imaging system was 2.7 μm/pixel.

2.4 Temperature calibration and image processing

The calibration curves were obtained from fluorescence images of the PDMS-RhB membrane acquired for a temperature range from 20 to 90 °C with intervals of 10 °C. Each image was acquired after achieving a steady temperature with the controller. The average time required to obtain an adequate thermal equilibrium for calibration purposes was approximately 10 minutes. Notice that this time constraint is due to the heater control system, and is not inherent to the thermal and fluorescence response of the membranes.

A temperature of 25 °C was selected as the baseline reading for all measurements. The PDMS-RhB membranes were exposed to laser excitation for 1 minute and during this time, 10 images along with their corresponding laser power were registered. In order to minimize possible quenching or bleaching effects, the incident laser light was blocked between measurements. The fluorescence intensity was analyzed considering an average intensity value calculated for each image using a gray scale conversion. This allowed us to obtain a ratio of the average fluorescence intensity (I) to the laser power (P) for each temperature; this ratio was then normalized using the ratio of the initial intensity to the initial laser power (I_0 / P_0), i.e.:

$$I_N = \frac{I / P}{I_0 / P_0}. \tag{1}$$

Notice that this normalization procedure accounts for average fluctuations in the laser power. Finally, the calibration curve was obtained plotting the normalized fluorescence intensity as a function of temperature.

3. Results and discussion

3.1 PDMS-RhB membranes: calibration and performance

The fabrication process mentioned above allowed us to obtain large PDMS-RhB membranes whose dimensions are limited by the size of the mold. For our experiments, we fabricated membranes with a maximum area of 20 mm by 70 mm and a thickness of 300 μm ± 30 μm. In contrast to other methods, the process to fabricate the membranes allowed us to embed the

Optical Materials EXPRESS

dye without the need of additional functional molecules or without any special doping procedures [9,13]. Furthermore, our method allowed for making custom size membranes that could be subsequently cut to predetermined sizes and shapes. For our experiments, we used square samples of 5 mm by 5 mm.

An optical microscopy image of a PDMS-RhB sample is shown in Fig. 2(a), exhibiting the nearly homogeneous color appearance of the fabricated membranes. Using a larger magnification, we were able to resolve clusters of RhB, which were most likely formed during the manual mixing performed in the last step of the fabrication procedure [18]. Nonetheless, the samples presented a fairly homogeneous fluorescence when irradiated with the laser. The optical absorption peak of the membranes was centered at around 545 nm, while the emission peak was located at 563 nm, as seen in the spectrum shown in Fig. 2(b), obtained with a high-resolution spectrometer (Ocean Optics, HR4000, 0.12 nm resolution).

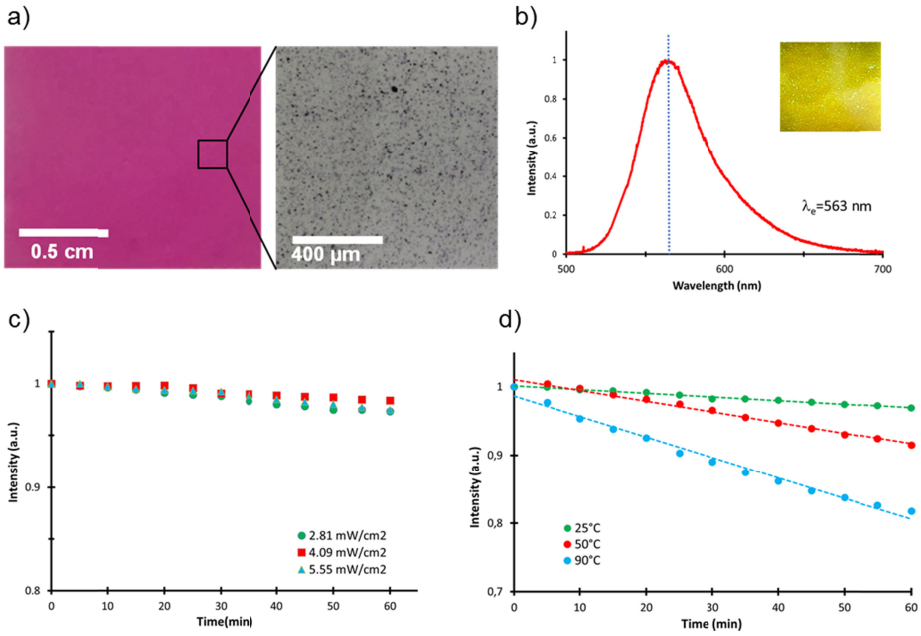

Fig. 2. PDMS-RhB membranes: (a) optical microscope image of the membranes; (b) typical emission spectrum and fluorescence emission (inset); (c) photobleaching effect in the membranes after 1 hour of laser exposure; (d) thermal bleaching after 1 hour for different temperatures.

Before testing the PDMS-RhB membranes for temperature measurements we assessed their stability. First, we evaluated if long exposures to laser light could cause degradation of the RhB and/or photobleaching, which is known to yield false temperature readings [2–4]. The laser intensity was fixed at 2.8 mW/cm^2 and the fluorescent signal was measured every 10 minutes during one hour. The average intensity was then analyzed in each set of images and the procedure was repeated for two different laser intensities (4.0 mW/cm^2 and 5.6 mW/cm^2). As shown in Fig. 2(c), the fluorescence showed only a small decay during this period of time (<3% approximately); hence, photobleaching does not seem to affect considerably the emission of the membranes, at least for the optical powers used for these measurements.

We also evaluated the thermal stability of the membranes upon monitoring the fluorescence intensity while keeping the samples at different temperatures (25 °C, 50 °C and 90 °C) during one hour. As shown in Fig. 2(d), the fluorescence intensity decayed linearly over time for a fixed temperature. Because the fluorescence intensity of RhB depends

Optical Materials EXPRESS

strongly on temperature, a faster decay is readily observed for higher temperatures. This behavior suggests that a slow degradation of the fluorescent dye occurs over time, which is consistent with previous reports on thermal cycling of dry RhB [4]. From Fig. 2(d), it is evident that the decay rate of the plots (i.e., the slopes) increases with temperature. Using the data in Fig. 2(d), the change in the decay rate of the intensity as a function of temperature was estimated to be $4x10^{-5}$ /°C. This thermal bleaching effect is evidently important in experiments involving long exposure times, although it can be accounted for during the calibration procedure upon increasing the temperature of the samples every 10 minutes. This yields a correction factor that can be applied during image processing to obtain the temperature map.

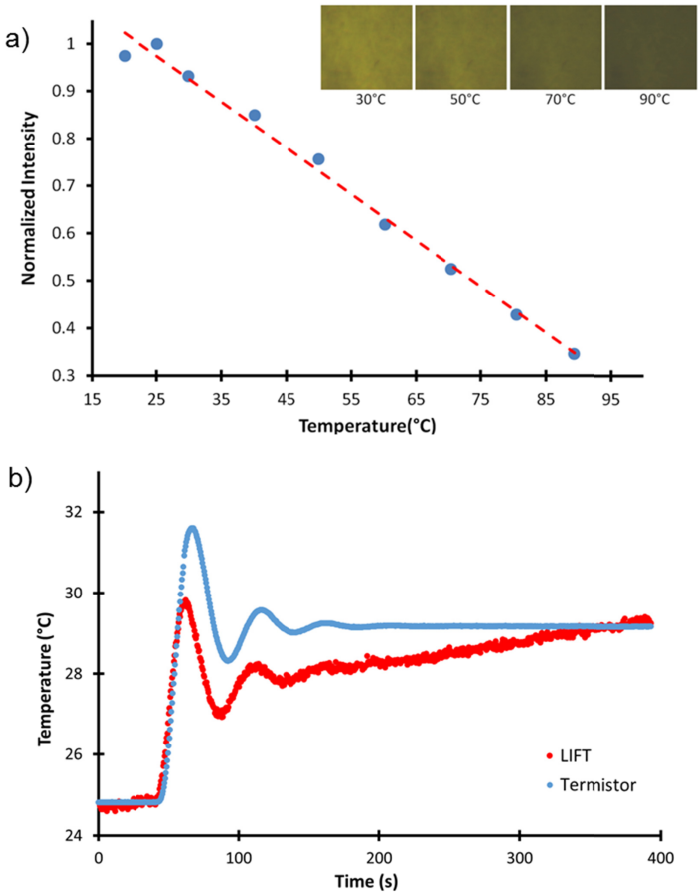

Fig. 3. (a) Calibration curve (normalized intensity vs. temperature) for the PDMS-RhB membrane. The insets show fluorescence images captured within the analyzed region (1.35 x 1.35 mm) for different temperatures. (b) Comparison of the temperature obtained with LIFT analysis and the temperature measured with the thermistor.

The calibration curve for temperature measurements was obtained upon analyzing the change in fluorescence intensity of the PDMS-RhB membrane as a function of temperature. Data were acquired for a temperature range of 25 to 90 °C, and as shown in Fig. 3(a), the normalized fluorescence intensity decreased in a linear fashion. This linear trend is similar to that observed in previous reports for dry layers of RhB [4] and for thin films of PDMS-RhB fabricated with other procedures [9,13]. The response time of the membranes was obtained after increasing the temperature with the PID controller (Fig. 3(b)). For comparison, the plot also shows the temperature registered by the thermistor used in the controller. The

Optical Materials EXPRESS

temperature obtained from the fluorescence of the membranes showed a similar trend as the data from the thermistor, albeit providing a lower reading. Hence, the fluorescence can readily track the temperature changes, however, an accurate temperature reading can only be obtained after the emission has reached a steady state value. From Fig. 3(b), a stable temperature reading in the thermistor occurs at approximately 200 s, while the fluorescence reading reaches a steady value at around 350 s, yielding a settling time of 2.5 min to obtain an accurate temperature reading. We attribute this limitation to the low thermal conductivity of PDMS host matrix (0.15 $Wm^{-1}K^{-1}$), which is known to impose some constraints when using PDMS in applications involving heat transfer phenomena [9,18]. Similar response times have been reported when using PDMS functionalized with RhB [9]; in contrast, to previous reports, our fabrication method involves only simple mixing without requiring any chemical process to incorporate the RhB in the host matrix.

3.2 Application to micro-thermometry: characterization of optical fiber micro-heaters

Optical fiber micro-heaters (OFMHs) are devices fabricated with layers of absorbing materials deposited on the tip of optical fibers; these photothermal devices are capable to increase the temperature in a highly localized manner [17,19]. Because they are made with standard optical fibers (125 μm diameter), the cross-sectional area of these heating elements is within a few hundred microns. The absorbing layer is deposited on the output end of the fiber and laser light (typically a laser diode) is then launched at the opposite end. Heat is subsequently produced and dissipated in the vicinity of the tip of the device. From previous reports, it is known that the increase in temperature in the vicinity of OFMHs is proportional to the optical power launched into the fiber [19]. However, information of the temperature distribution within the small area heated by these devices becomes relevant for applications involving biological tissue [17]. We therefore explored the feasibility to obtain the temperature maps in the surroundings of an OFMH using the PDMS-RhB membranes and LIFT.

For our experiments, we used OFMHs based on gold nanolayers, which have been previously reported to induce thermal damage in soft tissue [17]. The device was placed in physical contact with one edge of a PDMS-RhB membrane (see Fig. 4(a)). We first acquired 10 reference images at 25 °C, which were averaged and used to obtain the intensity reference ratio for each pixel. Subsequently, for each of the laser diode powers used in the test, 10 images were acquired and averaged and these were then used to estimate the intensity ratio for each pixel. The normalized intensity was then obtained upon dividing the intensity ratio by the reference ratio for the same pixels [3]. Finally, this normalized intensity was converted to temperature using the calibration curve for the membrane, thus yielding an image of the temperature distribution around the OFMH. A graphic depiction of this process is shown in Fig. 4(b). The images shown in Fig. 4(c) were obtained directly from the PDMS-RhB membranes for different powers of the laser diode; a decrease in fluorescence intensity is apparent in the vicinity of the OFMH, located at the bottom of the membrane as depicted in the images. Furthermore, as suggested by the dark areas in the images, the fluorescence intensity seems to be lower for higher powers of the laser diode.

The temperature maps obtained after processing the fluorescence images (Fig. 4(c)) are shown in Fig. 4(d). Clearly, the heat produced by the OFMH is dissipated around the OFMH tip; notice also that the registered temperature increases with the optical power, as previously reported for these devices [17,19]. Interestingly, the heated region seems to be smaller than one millimeter. For this particular case, the OFMH reached a maximum temperature of 78 °C and the total heated area was 750 μm x 650 μm. Using additional image processing, we can further estimate the temperature within a defined region of interest within the image. As an example, Fig. 4(e) shows the average temperature in a region close to the OFMH tip (80 μm X 80 μm) delimited by the red square in the temperature map shown in Fig. 4(d). As

Optical Materials EXPRESS

confirmed by the linear fitting, the average temperature was proportional to the optical power launched into the OFMH.

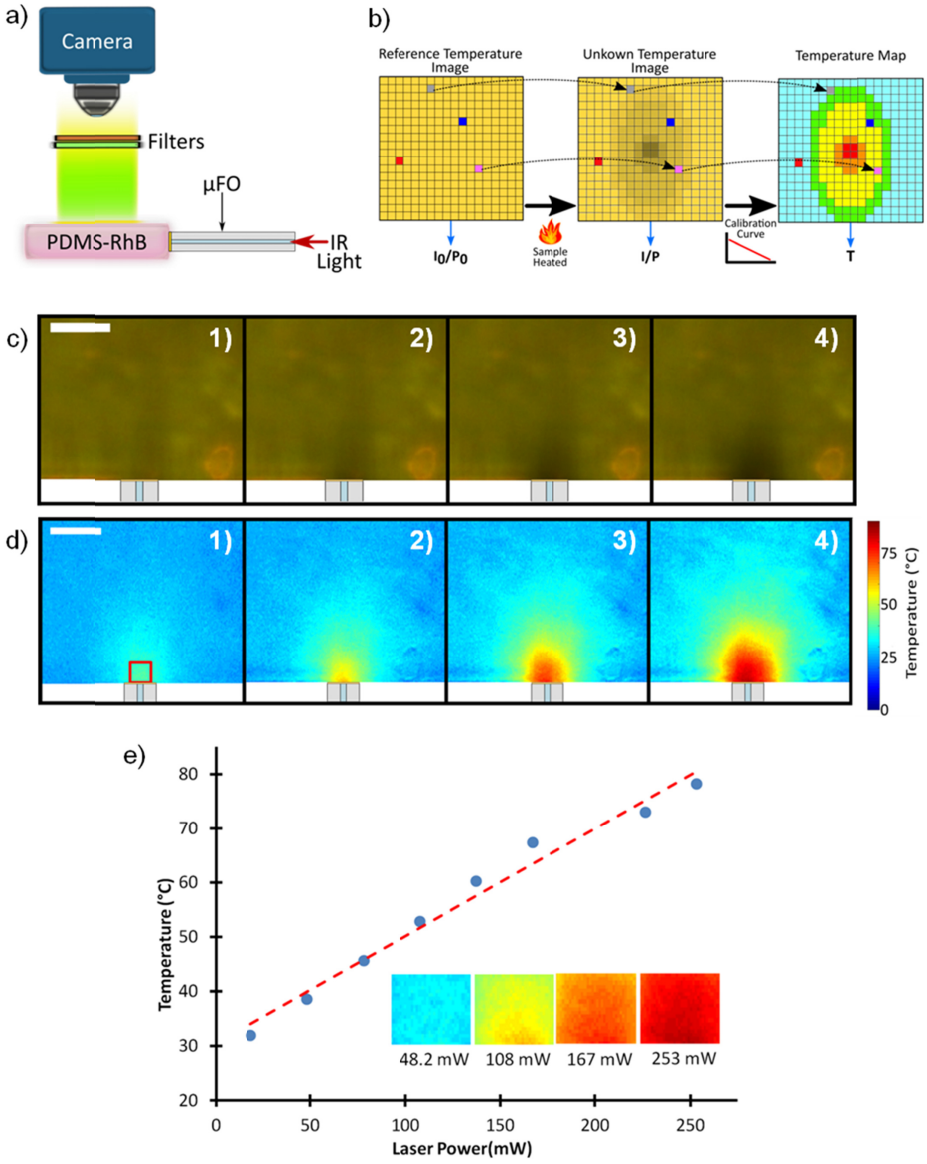

Fig. 4. Characterization of optical fiber micro-heater (OFMHs): (a) experimental setup to obtain the temperature maps in the vicinity of an OFMH with a RhB membrane and LIFT; (b) graphic depiction of the process used for obtaining the temperature maps; (c) fluorescence images from the membranes for different temperatures before processing (the location of the OFMH tip is illustrated at the bottom part of the images); (d) temperature maps obtained for laser diode powers of: (1) 48.2 mW, (2) 108 mW, (3) 167 mW and (4) 253 mW; (e) average temperature as a function of optical power evaluated for the region delimited by the red rectangle shown in 4(d). The scale bar is 200 μm.

In order to discard any effects due to IR radiation exiting the OFMH on the temperature readings, we also obtained temperature maps using pristine optical fibers (i.e., without the gold nanolayer at the tip). For these measurements, an additional filter was used to block any residual light from the laser diode. The temperature maps obtained for both, the pristine fiber

Optical Materials EXPRESS

and an OFMH are shown in Fig. 5. Since the PDMS and the RhB are both transparent for the IR wavelength [9], no increase in temperature is registered for the pristine fiber. Any IR contributions to the temperature measurements can therefore be discarded.

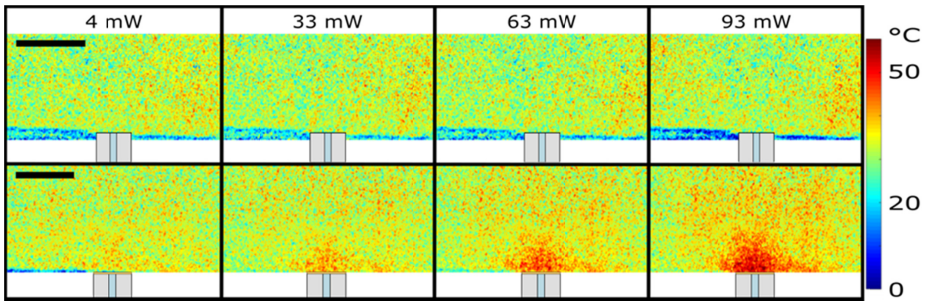

Fig. 5. Temperature maps for different optical powers obtained with a pristine optical fiber (top) and with an OFMH (bottom). The scale bar is 200 μm.

Limitations for the temperature resolution achievable with this technique are mostly related to the gray scale conversion during image processing. Because the gray levels available for each pixel limit the minimum intensity that can be detected, camera features such as sensitivity and noise represent the ultimate temperature resolution that can be achieved. In principle, with our experimental setup, the camera can provide a temperature resolution of less than 1°C. Another limiting factor is the sensitivity of the membranes to temperature changes. As shown in our characterization experiments, the response of the membranes is susceptible to degradation mostly due to thermal quenching (see Fig. 2(d)). This affects directly the sensitivity as well as the resolution of the temperature measurements. Nonetheless, this factor can be accounted for following the calibration procedure described before. Regarding the spatial resolution, this is limited by the microscope objective used for image acquisition. Scattering effects within the membrane due to RhB clustering will also play a role in limiting the spatial resolution. The noise observed in Fig. 5, for example, is mostly due to the RhB clusters produced while fabricating the membranes (see Fig. 2(a)). However, we believe that clustering can be avoided following simple mixing procedures such as those previously reported for the fabrication of photothermal membranes [18].

4. Conclusions

We have demonstrated that PDMS-RhB membranes can be used to measure temperature through LIFT. Using this technique together with the proposed membranes we were able to analyze the fluorescence emitted by membranes and captured by a CMOS camera. The membranes used in our experiments allowed us to determine temperature maps in the range from 25 °C to 90 °C, with a temperature resolution of about 1 °C. The spatial resolution of our measurements is approximately 2.7 μm/px, which is adequate for acquiring temperature maps in processes requiring micron resolution measurements. Moreover, these membranes allow for performing temperature measurements in dried samples in a non-destructive manner, without compromising the sample of interest. LIF thermometry performed with PDMS-RhB membranes was used to obtain the temperature map around OFMH devices, which are of interest for photothermal applications. Our results showed that the heat generated by OFMH is proportional to the optical power of the laser light launched into the fiber, and the heat generated is highly localized within a spatial region of less than one millimeter. The use of temperature sensitive membranes may extend the use of LIFT in applications involving the characterization of thermal devices with high spatial resolution.

Optical Materials EXPRESS

Funding

DGAPA-UNAM (PAPIIT IT101215); Conacyt-FONCICYT (246648); National Science Foundation (NSF) (NSF-PIRE 1545852, NSF-EAGER 1547014).

Acknowledgements

JHC acknowledges support from PASPA-DGAPA-UNAM and from Conacyt during his sabbatical at UCR. The authors would like to thank Carlos David Ramos Vilchis for his technical support and Prof. Carlos Palacios for his technical comments on the LIFT processing technique.